JOURNAL OF APPLIED ELECTROCHEMISTRY 10 (1980) 535–541

Structure and corrosion resistance of electrolytic nickel coatings containing codeposited nonconducting particles

ST. RASHKOV, N. ATANASSOV

Institute of Physical Chemistry, Bulgarian Academy of Sciences, Sofia 1040, Bulgaria

Received 3 September 1979

The codeposition of nonconducting silicate particles with different grain size during the plating of nickel coatings with preferential orientation along with ⟨2 1 1⟩ axis is investigated by electron microscopy. The results confirm that small size particles, about 20 nm, are included in the twinning defects, inherent to this orientation, blocking the latter as active dissolution sites. Larger particles, approximately 1.5 μm, are included in the bulk of the coating, and cause a continuous redistribution and decrease of the corrosion rate. On the other hand, when particles of 20 nm size are used, an unusual decoration of the twinning plane {1 1 1} perpendicular to the substrate, may lead to the elucidation of some theoretical problems related to the initiation of the texture ⟨2 1 1⟩. A dissolution mechanism is proposed, based on the mutual effect of both factors: redistribution of the corrosion current, and blocking of the twinning planes which act as active dissolution centres. This mechanism is confirmed by Corrodkote tests of codeposited nickel coatings.

1. Introduction

In recent years there has been an increasing use of microporous chromium plates for protective–decorative copper–nickel–chromium coatings. This is due to the fact that the corrosion resistance of the system is increased several times as compared with the conventional triplex bright plates, which require a substantial thickness of the nickel layer.

From the first papers of Odekerken [1, 2] several publications in this field deal with the nature, shape, structure, and dimensions of the non-conducting particles [3–6], the mechanism of inclusion in the coating [7–12], the number of particles included as a function of deposition conditions, the stability of the respective suspensions [13–16], etc. Special attention has been devoted to the relation between the corrosion resistance of the multilayer system copper–nickel–chromium, and the number of pores in the chromium layer [2, 13, 17–19]. The excellent corrosion resistance of the complex coating which used a several micron thick intermediate nickel layer with non-conducting inclusion particles is due to the extensively increased nickel surface as a result of the large number of micropores in the adjacent chromium layer. Thus the corrosion current with respect to the nickel plate decreases substantially.

Probably this generally accepted view (which is supported by data derived from practical applications) has discouraged investigations aimed at the determination of the effect of the structural peculiarities of the nickel coating, the pattern by which the nonconductive particles are included and their nature, upon the corrosion resistance of multilayer copper–nickel–chromium plates.

The present paper is aimed at the investigation of the inclusion of nonconductive particles with different grain size in electrolytically deposited nickel coatings with a definite structure, and to find a possible relationship between the inclusion pattern of the particles, the structural peculiarities of the nickel plate, and the corrosion behaviour of the copper–nickel–chromium system.

2. Results and discussion

The investigated coatings were deposited in a Watts electrolyte in the presence or absence of brighteners. The size of the nickel crystallites was approximately 70–80 nm in the former case, and 1.5 μm in the latter.

0021–891X/80/040535–07$02.70/0

Fig. 1. CEM photographs of nickel coatings with texture ⟨2 1 1⟩ (×6500).

The coatings were electrodeposited under galvanostatic conditions at 3–5 A dm^{-2}, temperature 50–60° C, pH 4.5 and displayed a ⟨2 1 1⟩ texture. The nonconductive particles were of a silicate nature activated in an effort to improve their surface properties and increase the stability against sedimentation of the electrolyte–particle suspension. They were separated according to grain size so as to obtain fractions with predominant dimensions approximately 5 μm, 1.5 μm and maximum 200–300 nm. The coatings were checked by conventional CEM scanning, SEM and transmission TEM electron microscopy at high accelerating voltages. The methods for the preparation of the samples of thin foils subjected to irradiation are described in detail in a previous paper [20]. A version of the electro-jet method [21, 22] for stripping nickel foil in acetic (77%) and perchloric (23%) acid solutions at 12 V was used throughout. This technique offers the possibility of investigating the development at different stages of growth; thus the results that are obtained apply to a distinct and defined thickness layer.

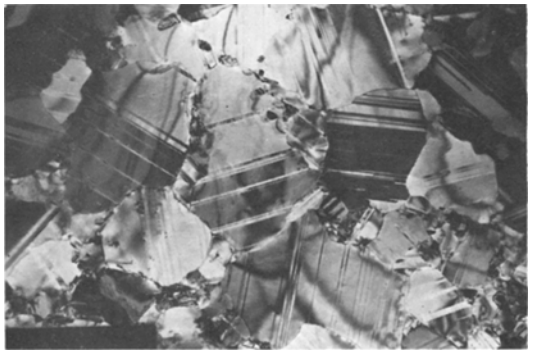

Fig. 2. TEM photograph of nickel coating with texture ⟨2 1 1⟩ (×13 000).

The inclusion of particles with grain size approximately 1.5 μm in nickel coatings of different thickness was investigated. According to the data published in our previous papers [20, 23] nickel coatings which have the texture ⟨2 1 1⟩, regardless of their thickness are composed of pyramid-shaped crystallites with binary symmetry (Fig. 1), characterized by the presence of twinning planes {1 1 1}, perpendicular to the substrate (Fig. 2).

Fig. 3 gives the SEM data of 0.5, 3 and 10 μm thick coatings. Samples 0.5 μm thick (Fig. 3a) display a fine grain structure. With an increase of the thickness to 3 μm or 10 μm (Fig. 3b, c) the size of the crystallites increases, and at 10 μm one can see distinctly the agglomerates formed by the coverage of the nonconductive particle with pyramid-shaped crystallites. In order to clarify further the inclusion process under conditions similar to practical application, larger 5 μm particles were used for inclusion in bright coatings with a crystallite size of approximately 70 nm, and thickness 15 μm. Fig. 4a shows numerous round-shaped particles which have not coalesced. At increased magnification, the separate particles are distinctly visible (Fig. 4b) and the different stages of formation and sealing of the pores in the coating, depending on the size of the particles, can be observed (Fig. 4c).

In a previously published paper [24] we discussed the corrosion behaviour of the multilayer copper–nickel–chromium system with particle-codeposited nickel. The tests were carried out by the Corrodkote [25] method, which gives the corrosion resistance of the coating expressed in grades (the highest grade 10 corresponds to an absence of corrosion) as a function of the duration of exposure (one cycle is 20 h). Fig. 5 [24] suggests that regardless of the fact that the thickness of the nickel in the codeposited nickel–chromium (curve 3) is 2 to 3 times less than that conventionally used (curve 2) and both samples have an approximately equal number of pores on the surface, the corrosion resistance of both systems is very high. Therefore it can be seen that some other factors affect the corrosion resistance of the system, and they are not related to the number of micropores on the surface. Such factors might be structural peculiarities of the nickel coating used, e.g. defect sites in the crystal struc-

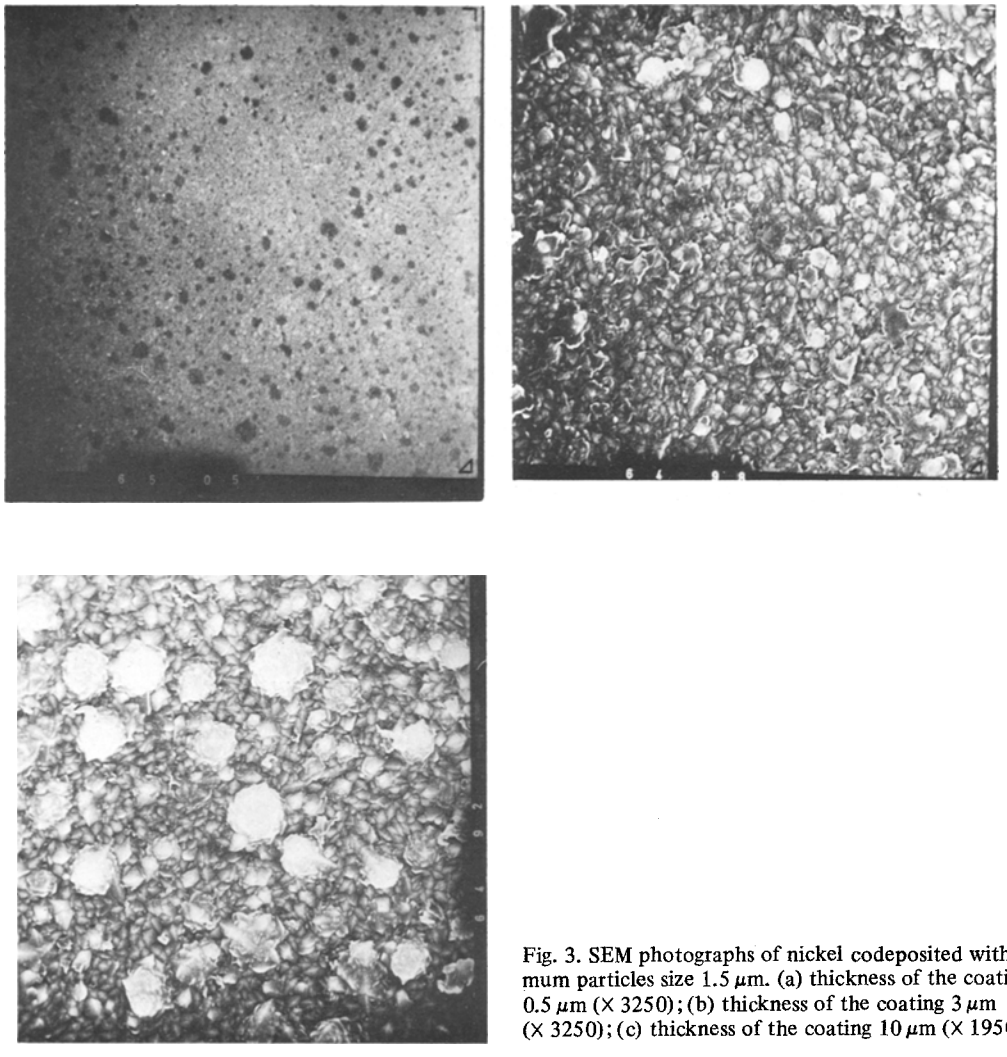

Fig. 3. SEM photographs of nickel codeposited with maximum particles size 1.5 μm. (a) thickness of the coating 0.5 μm (× 3250); (b) thickness of the coating 3 μm (× 3250); (c) thickness of the coating 10 μm (× 1950).

ture which act as active dissolution centres, or the redistribution of the corrosion current in the bulk of the coating containing included particles, provided thickness is more than 7 μm.

The most commonly used nickel seal coatings with thickness up to 3 μm are deposited from baths containing 1,4-butyn-2-diol as brightener.

According to some investigations, in the presence of 1,4-butyn-2-diol at 50° C, and above 3 A dm^{-2} (conditions similar to routine applications) the nickel coatings display a ⟨2 1 1⟩ texture [23, 26] i.e. the texture is identical with that obtained in a pure Watt's electrolyte, but the size of the crystallites is substantially smaller, 70 nm. Fig. 6 clearly show that in this case also the twinning planes {1 1 1} are perpendicular to the substrate.

Since the twinning planes {1 1 1} perpendicular to the substrate surface are the active sites of growth and dissolution [27, 28], it was very interesting to check whether the nonconducting particles used in our experiments will be predominantly included in these defective sites, at the grain boundaries, or will be uniformly distributed in the bulk of the coating. Model studies were carried out by the co-deposition of nickel coatings in a Watt's electrolyte with texture ⟨2 1 1⟩ and grain size 1.5 μm when the twinning planes are very distinct, while the nonconducting particles are fine-grained (up to 200 nm,

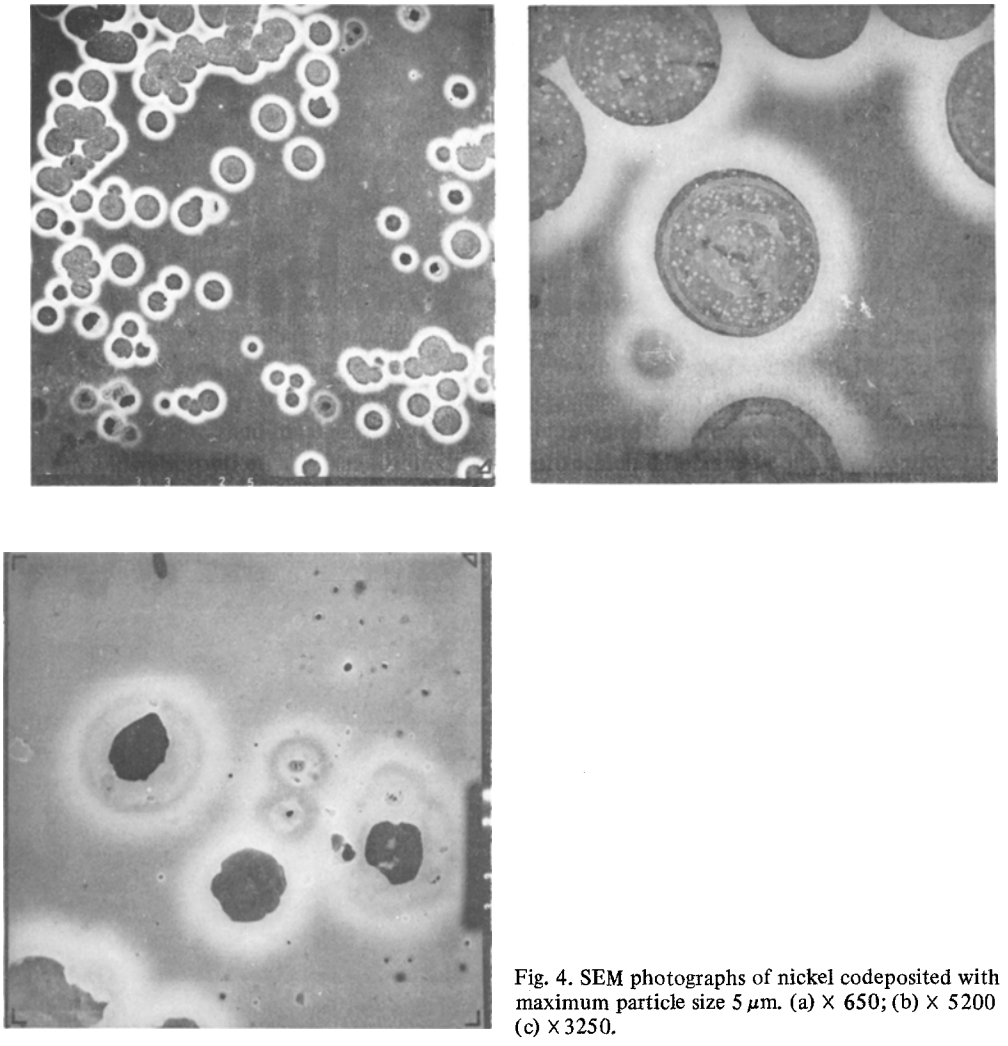

Fig. 4. SEM photographs of nickel codeposited with maximum particle size 5 μm. (a) × 650; (b) × 5200 (c) × 3250.

predominantly 20–30 nm). The results of the investigations presented in Fig. 7 show that the particles are included mainly at the twinning planes {1 1 1} and less in the bulk of the crystallites and the grain boundaries.

Consequently the twinning planes {1 1 1} are active sites for the inclusion not only of nickel ions [27], but also particles. Therefore it may be presumed that this preferential inclusion of the nonconductive particles can block the twinning planes which are active centres of dissolution thus decreasing the corrosion rate.

The use of a goniometric accessory showed that when we swivel the object to a certain degree, some of the twinning planes disappear since they are not in a reflecting position, but one can observe distinctly the particles which decorate them. By the use of this peculiar decoration mode, the exact number of twinning planes {1 1 1} perpendicular to the substrate can be established. However it must be stressed that the extent of inclusion of the particles varies, which suggests a difference in the activity of the twinning planes.

The effect upon the dissolution pattern caused by the blocking of the twinning planes by the particles was studied by plating nickel coatings from a Watt's bath under identical conditions in the presence or absence of particles. The samples were subjected to 90 s anodic etching in an ethyl alcohol–phosphoric acid electrolyte at current density of 2 A dm^{-2}, followed by CEM investigations.

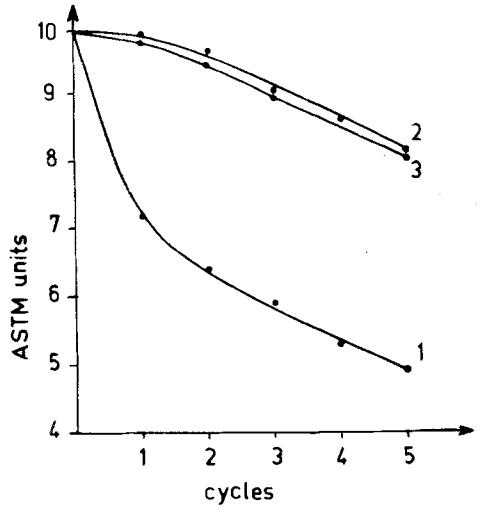

Fig. 5. Change in the corrosion resistance with time according to the 'corrodkote' test. Curve 1, bright nickel 28 μm thick and chromium 0.5 μm; curve 2, bright nickel 25 μm thick, codeposited nickel 3 μm and chromium 0.5 μm; curve 3, codeposition nickel with thickness 10 μm chromium 0.5 μm.

Fig. 8a shows clearly that in a coating free of particles, the twinning planes are the active sites of dissolution, while in the presence of particles (Fig. 8b) this phenomenon is not observed and the coating dissolves uniformly. Therefore it is likely that the inclusion of particles leads to the blocking of the active sites and dissolution proceeds slowly, due to this 'inhibitive' effect.

It is quite possible that this phenomenon is present in the nickel coating with the same texture and very fine-grained structure, i.e. a case very similar to the practical applications, as for instance

Fig. 7. TEM photographs of nickel codeposited with particle size 20 nm at 1 MeV (× 65 000).

with the addition of 1,4-butyn-2-diol to the electrolyte.

The results presented up to now suggest that the particles with different size are included at definite sites in the nickel coating, thus affecting in a different way the improvement of the corrosion resistance of the system: coarse grains create pores in the bulk, while fine-grained particles block the active sites of dissolution.

It is of interest to examine the probable development of corrosion in 10–15 μm thick nickel coatings containing particles and compare it with the routine 3 μm thick nickel coating containing included particles and 25 μm bright nickel. In the case of a 3 μm coating it is generally accepted that corrosion starts from the micropores, and due to their large number, the corrosion current is distributed uniformly on the surface of the nickel plate. With the broadening of the corrosion pits in the nickel layer, possibilities are created for the

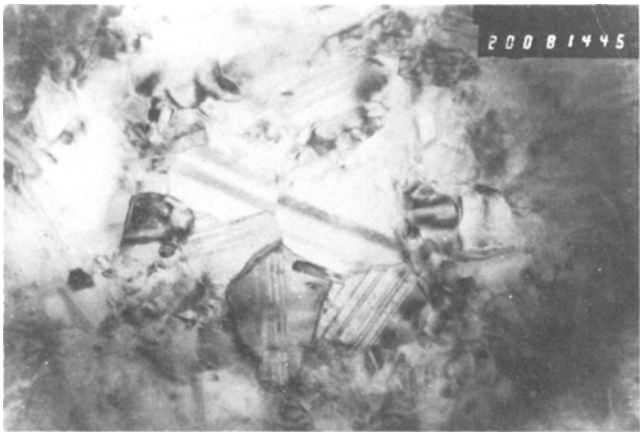

Fig. 6. TEM photographs of nickel coatings with texture ⟨2 1 1⟩ deposited in the presence of butyn-2-diol-1,4 (× 195 000).

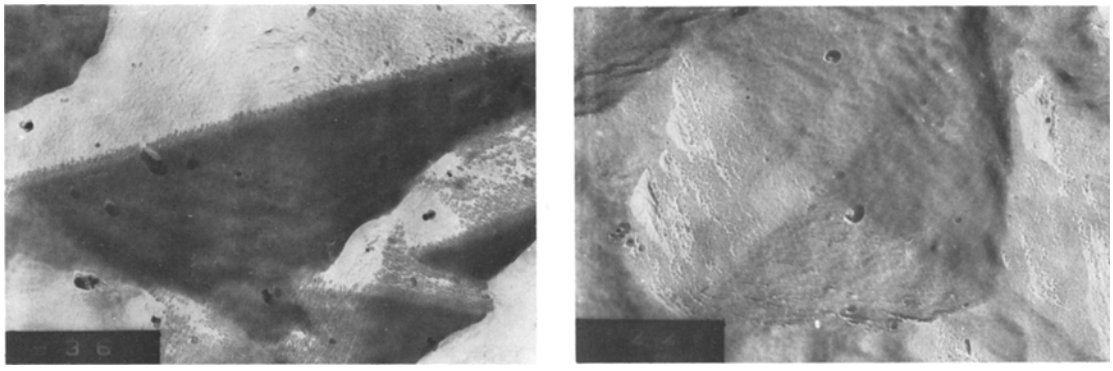

Fig. 8. (a) CEM photographs of nickel coatings after anodic etching (× 32 500); (b) CEM photographs of nickel codeposited with particle size 20 nm after anodic etching (× 32 500).

corrosion process to reach the substrate, due to the substantial number of active centres of dissolution (the {1 1 1} planes perpendicular to the substrate).

Nickel coatings 10–15 μm thick containing particles show that the initial corrosion also starts at the micropores and since in this case the twinning planes are blocked, the corrosion process should develop slowly along the metal–particle boundary. Fig. 9 shows that when a particle containing nickel foil is stripped and becomes thinner, dissolution really occurs around the particles, i.e. the metal–particle boundary is an anodic region. Since the number of particles in the bulk of the coating is enormous, probably due to the penetration of the corrosion process in depth, a continuous redistribution of the corrosion current occurs on an ever increasing anodic area. This in the long run leads to a substantial suppression of the corrosion rate.

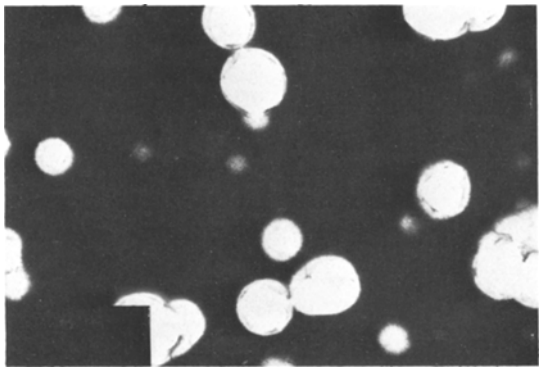

Fig. 9. TEM photographs of nickel codeposited with particles having maximum size 1.5 μm after disolution (× 6500).

This mechanism, regardless of the fact that under normal conditions sulphur-containing organic additives are also present (leading to sulphur inclusions in the coating) is confirmed to a certain extent by the experimental results in Fig. 10 which shows the change in the corrosion resistance with time carried by the 'corrodkote' test method. These data suggest that in the system 10 μm bright nickel and 3 μm nickel containing particles, corrosion starts rapidly (curve 1) when compared with a 10 μm thick plate, which contains numerous inclusion particles in the bulk (curve 2).

Future investigations will investigate the mechanism in greater detail.

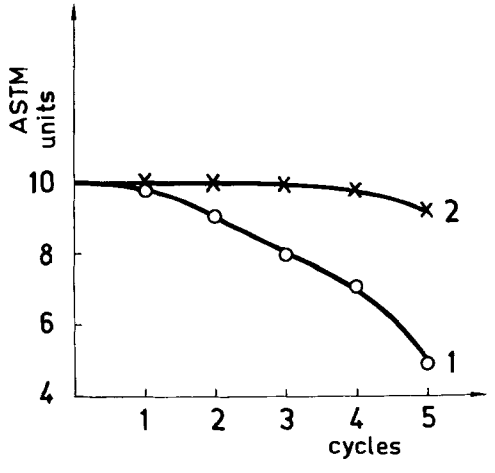

Fig. 10. Change in the corrosion resistance with time according to the 'corrodkote' test. Curve 1, bright nickel 10 μm thick, codeposited nickel 3 μm, chromium 0.3 μm, chromium 0.3 μm; curve 2, nickel codeposited with thickness 10 μm, chromium 0.3 μm.

References

[1] J. M. Odekerken, *Metall.* **16** (1962) 17.
[2] *Idem, Ibid* **18** (1964) 70.
[3] R. S. Seyfullin, *Tr. KHTI* **30** (1962) 253.
[4] H. Brown and H. Silamm, *Trans. Inst. Met. Fin.* **42** (1974) 50.
[5] W. Metzger and H. Florian, *Oberflächen technik* **52** N3-4 (1975) 45, 48.
[6] T. Hayashi and N. Maeda, *Interfin. 76, Tagungsberichtsb. Weltkongr. Oberfläch Behand Met. 9th* (1976) Pep. 18, 14.
[7] F. K. Sauter, *J. Electrochem. Soc.* **110** (1963) 557.
[8] T. Tomaszewski, L. Tomaszewski and H. Brown, *Plating* **56** (1969) 1234.
[9] J. Foster and A. Kariapper, *Trans. Inst. Met. Fin.* **51** (1973) 27.
[10] D. W. Snaith and P. D. Groves, *ibid* **50** (1972) 95.
[11] N. Guglielmi, *J. Electrochem. Soc.* **119** (1972) 1009.
[12] Ju. Ju. Matulis, D. K. Ramanauskene and N. S. Perene, Sb 'Nadejd. i dalgowznost. det. i mashin' Krasnojarsk (1974) 4.
[13] R. S. Seyfullin and F. I. Nadeeva, *Tr. KHTI* **40** (1969) 71.
[14] N. Furukawa and T. Hayashi, *Kinz. Hyom. Giyzitusu* **28(10)** (1977) 527.
[15] W. Metzger, *Metall.* **32** (1978) 180.
[16] D. K. Ramanauskene, N. S. Perene, L. M. Sjarukaite and Ju. Ju. Matulis, *Tr. AN Lit. SSR, ser. B* 5 (1974) 61.
[17] R. S. Seyfullin, F. I. Nadeeva, W. N. Golowanov, L. Ja. Seliskaja and G. I. Alekseev, Sb. 'Zastitn pokr.w mashinostr.' Krasnoyarsk (1973) 39.
[18] E. A. Mamontov, B. G. Karnauhov, W. W. Okulov and Ju. W. Kojemjakin, *Tez. dokl. VIII Perm. konf. po zastita met.ot korr. 'Perm'* (1974) 127.
[19] R. J. Clauss, T. Tomaszewski and H. Brown, Pat. USA kl.204-41/c 23 b 5/08/N 3825478, (1974).
[20] N. Atanassov, St. Witkova and St. Rashkov *Izv.po chimia-BAN* **X** (1977) 247.
[22] G. W. Briers, D. W. Dame, M. A. Dewey and I. Brammer, *J. Inst. Met.* **93** (1964–65) 77.
[23] St. Rashkov and N. Atanassov, *Electrodep. and Surf. Treat.* **3** (1975) 105.
[24] St. Rashkov, N. Atanassov and all., *7 International Congress on Metal Corrosion* 44/11 Rio de Janerio (1978) p. 1812.
[25] ASTM Specification B380-61T.
[26] N. Atanassov, S. Shishkova, A. Kolev and St. Rashkov, *Izv.na otd.chim.nauki-BAN* **V** (1972) 409.
[27] M. Froment and G. Maurin, *J. de Microscopie* 7 (1968) 38.
[28] G. Raitchevski and T. Milusheva, *Zastita metalov* **XI** (1975) 558.